JCB Article

A subunit of the dynein regulatory complex in *Chlamydomonas* is a homologue of a growth arrest–specific gene product

Gerald Rupp[1,2] and Mary E. Porter[1]

[1]Department of Genetics, Cell Biology, and Development, University of Minnesota Medical School, Minneapolis, MN 55455
[2]Department of Anatomy, Southern Illinois University School of Medicine, Carbondale, IL 62901

The dynein regulatory complex (DRC) is an important intermediate in the pathway that regulates flagellar motility. To identify subunits of the DRC, we characterized a *Chlamydomonas* motility mutant obtained by insertional mutagenesis. The *pf2-4* mutant displays an altered waveform that results in slow swimming cells. EM analysis reveals defects in DRC structure that can be rescued by reintroduction of the wild-type *PF2* gene. Immunolocalization studies show that the PF2 protein is distributed along the length of the axoneme, where it is part of a discrete complex of polypeptides. PF2 is a coiled-coil protein that shares significant homology with a mammalian growth arrest–specific gene product (Gas11/Gas8) and a trypanosome protein known as trypanin. PF2 and its homologues appear to be universal components of motile axonemes that are required for DRC assembly and the regulation of flagellar motility. The expression of *Gas8/Gas11* transcripts in a wide range of tissues may also indicate a potential role for PF2-related proteins in other microtubule-based structures.

Introduction

Cilia and flagella are homologous, microtubule-based organelles found on diverse cell types ranging from spermatozoa to the epithelia lining the respiratory and reproductive tracts. The driving force for motility is supplied by the axonemal dynein ATPases. Defects in the dynein motors, accessory proteins that regulate dynein activity, or other components that control axoneme assembly have profound consequences. In vertebrates, these include infertility, respiratory and kidney disease, and defects in the determination of the left–right body axis during embryonic development (Afzelius, 1995; Nonaka et al., 1998; Sapiro et al., 2002; Pazour and Rosenbaum, 2002; for review see Supp et al., 2000). In motile axonemes, dyneins form the inner and outer arms that are bound to the outer doublet microtubules and interact transiently with adjacent doublet microtubules to generate the force for interdoublet sliding (for review see Kamiya, 2002). Because dyneins can generate sliding forces in only one direction (Sale and Satir, 1977; Fox and Sale, 1987), the activity of the dynein arms must be coordinated both spatially and temporally to generate an efficient flagellar waveform.

Both structural and genetic evidence have implicated the central pair (CP)* and radial spoke (RS) structures as key regulators of dynein activity. Mutations that disrupt the CP or RS structures result in flagellar paralysis under physiological conditions (Witman et al., 1978), by a mechanism that appears to involve global inactivation of the dynein arms (Huang et al., 1982; Smith and Sale, 1992). One hypothesis is that the CP projections act like a distributor that periodically sweeps past the RS heads during CP rotation, inducing a local signal that is ultimately transmitted to the dynein arms (Omoto and Kung, 1979; Omoto et al., 1999). In the absence of these signals, other axonemal components must inhibit dynein activity. Evidence for such an inhibitory control system has been obtained by the isolation of extragenic suppressor mutations that restore partial motility to CP/RS-defective strains without restoring the missing structures (Huang et al., 1982; Piperno et al., 1992). Two distinct groups of suppressor mutations have been identified. One group alters the activity of the outer dynein arms by mutations in dynein heavy chain domains that regulate cross-bridge activity (Huang et al., 1982; Porter et al., 1994; Rupp et al., 1996). The second group alters the assembly of the inner dynein arms and/or a

Address correspondence to Mary E. Porter, Department of Genetics, Cell Biology, and Development, 6-160 Jackson Hall, 321 Church St., SE, Minneapolis, MN 55455. Tel.: (612) 626-1901. Fax: (612) 625-4648. E-mail: mary-p@biosci.cbs.umn.edu

Key words: dynein; flagella; Gas8; Gas11; TLTF

*Abbreviations used in this paper: CP, central pair; DRC, dynein regulatory complex; EDC, 1-ethyl-3-(3-dimethylaminopropyl) carbodiimide hydrochloride; RS, radial spoke; TLTF, T lymphocyte triggering factor.

subset of closely associated polypeptides known as the dynein regulatory complex (DRC) (Huang et al., 1982; Piperno et al., 1992, 1994; Porter et al., 1992; Gardner et al., 1994). The mechanism by which the DRC regulates dynein activity is still unclear.

The DRC contains at least seven polypeptides that are tightly associated with the outer doublet microtubules (Piperno et al., 1994), but until this study, the identity of any of these DRC subunits has been unknown. The DRC has also been correlated with a crescent-shaped structure located near the base of the second RS, close to the site of attachment for the nexin link (Burgess et al., 1991; Mastronarde et al., 1992; Gardner et al., 1994; Woolley, 1997). This structure appears to be ideally situated to mediate local signals between the CP/RS complex, the nexin links, and the dynein arms, and it is altered or missing in DRC-defective strains (Mastronarde et al., 1992; Gardner et al., 1994). It is unclear whether the local signals that control dynein arm activity are chemical, mechanical, or both. However, both pharmacological and biochemical evidence suggest that ciliary and flagellar motility is regulated in part by reversible phosphorylation of axonemal components (for review see Porter and Sale, 2000). Several kinases and phosphatases are anchored in the axoneme (San Agustin and Witman, 1994; Yang and Sale, 2000; Yang et al., 2000; Gaillard et al., 2001; Smith, 2002), and numerous axonemal phosphoproteins have been detected (Piperno et al., 1981). Recent studies also show that components of the dynein arms are targets of reversible phosphorylation, and that changes in their phosphorylation state can modulate dynein activity and flagellar motility (Hamasaki et al., 1991; Habermacher and Sale, 1997; King and Dutcher, 1997; Yang and Sale, 2000).

To identify axonemal components that regulate dynein activity, we used insertional mutagenesis procedures in *Chlamydomonas* (Tam and Lefebvre, 1993) to recover "tagged" motility mutants with characteristics similar to previously described DRC mutants (Huang et al., 1982; Gardner et al., 1994). Structural, functional, and genetic evidence indicate that we have cloned the *PF2* locus, which encodes DRC subunit 4, a highly coiled-coil protein of ~55 kD that is tightly associated with the outer doublet microtubules. Localization of an epitope-tagged PF2 construct indicates that PF2 is uniformly distributed along the length of the axoneme and also associated with the basal body region. Interestingly, homologues of PF2 have recently been identified in diverse organisms, ranging from trypanosomes (trypanin) to humans (Gas8/Gas11), where they have been proposed to play important, but poorly understood, roles in both cell motility and growth arrest (Brenner et al., 1989; Hutchings et al., 2002; Yeh et al., 2002). Our study strongly suggests that these PF2/trypanin/Gas8/Gas11 homologues are part of a conserved DRC complex involved in the regulation of axonemal motility in multiple species. The presence of *Gas8/Gas11* transcripts in growth-arrested cells and tissues that do not assemble motile axonemes (Brenner et al., 1989; Whitmore et al., 1998; Yeh et al., 2002; unpublished data) may also indicate a possible role for the DRC in other microtubule-based organelles.

Results

Recovery of a tagged *pf2* allele

A collection of motility mutants generated by insertional mutagenesis was screened for strains with abnormal swimming behaviors to identify new loci involved in the regulation of motility. One strain, 9B11, swam more slowly than wild-type cells (~51 ± 14 μm/s vs. 139 ± 24 μm/s) and displayed an aberrant flagellar waveform similar to those seen in inner arm and DRC mutant strains (Brokaw and Kamiya, 1987; Gardner et al., 1994). Direct comparison between different strains by phase contrast microscopy indicated that 9B11 was most similar to the DRC mutant *pf2*. 9B11 was backcrossed to a nit^- strain with wild-type motility to verify that the 9B11 motility defect was linked to the *NIT1* gene used as a selectable marker. Analysis of the tetrad progeny confirmed that the 9B11 motility phenotype cosegregated with the nit^+ phenotype (<6.3 cM apart).

Cloning and characterization of the *PF2* gene

To identify the gene that was disrupted in 9B11, a fragment of genomic DNA flanking the site of plasmid insertion was obtained by screening a size-fractionated minilibrary with a probe derived from the 3′ end of the *NIT1* gene (see Materials and methods; Fig. 1 A). Southern blots of wild-type and 9B11 genomic DNA probed with the flanking DNA (flanking clone 1 [FC-1]) confirmed that this DNA was located near the site of the mutation in 9B11 (Fig. 1 B).

FC-1 was then used to screen a wild-type library and recover more than 30 kb of genomic DNA (Fig. 1 C). RFLP mapping procedures revealed that this DNA was closely linked to the *PF2* locus on linkage group XI (see Materials and methods). These results and the 9B11 motility phenotype described above suggested that 9B11 might represent a new *pf2* mutation. To test if any of the phage clones contained a full-length copy of the *PF2* gene, three clones were analyzed for their ability to rescue the 9B11 and *pf2* motility defects by cotransformation. Two clones, λG2 and λJ1, were able to restore wild-type motility to either 9B11 or *pf2-1* cells (Fig. 1 C). The 9B11 strain was therefore renamed *pf2-4*. The λM2 clone, which shares ~50% overlap with λG2, failed to rescue the motility defects, suggesting that the *PF2* gene must extend beyond the limits of this clone.

Selected restriction fragments from the phage clones were used to probe Southern and Northern blots to define the boundaries of the *PF2* gene. Genomic Southern blots probed with subclones A–D indicated that the *NIT1* plasmid inserted into a 3.5-kb SacI restriction fragment without significant deletion of the surrounding genomic DNA in *pf2-4* (Fig. 2 A). Subclones A–D were also hybridized to Northern blots loaded with total RNA isolated from wild-type and mutant cells both before and 45 min after deflagellation to delineate the boundaries of the *PF2* transcription unit and determine the size of the *PF2* transcript. Deflagellation has previously been shown to induce up-regulation of transcripts that encode flagellar proteins (for review see Lefebvre and Rosenbaum, 1986). Probes B–D identified a single ~2.5-kb transcript that was up-regulated after deflagellation in wild-type cells and missing in

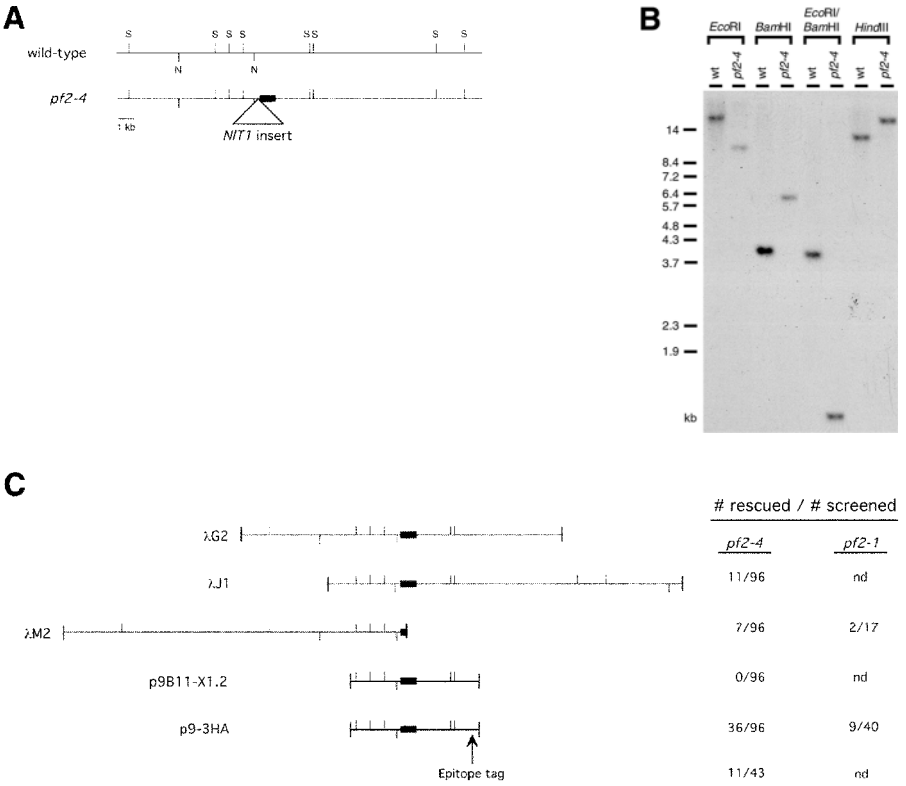

Figure 1. **Cloning the *PF2* gene.** (A) Partial restriction maps of the region containing the *PF2* gene from wild-type and *pf2-4* (9B11). Also indicated is the location of the *NIT1* plasmid insertion in 9B11, now known as *pf2-4*, and the position of the flanking clone FC-1 (black box) representing the NotI/BamHI restriction fragment recovered from the 9B11 minilibrary. S, SacI sites; N, NotI sites. (B) Southern blot of wild-type (wt) and *pf2-4* genomic DNA digested with the indicated restriction enzymes and hybridized with FC-1. (C) Alignment of three overlapping phage clones recovered with FC-1 (black boxes) and two plasmid clones, derived from λG1, that contain the *PF2* gene. Plasmid p9-3HA is the epitope-tagged *PF2* construct. Also shown are the number of rescued strains obtained by cotransformation of *pf2-4* and *pf2-1* with the selected clones. nd, not determined.

pf2 strains (Fig. 2 B). Given the location of the *NIT1* insertion in *pf2-4* and the expression pattern of the 2.5-kb transcript, we identified this region as the site of the *PF2* transcription unit. Probes A and B also hybridized to a smaller ~2.2-kb transcript that was expressed in both wild-type and *pf2* cells and showed homology to a 50S ribosomal subunit (Fig. 2 A).

The *PF2* transcription unit contains 12 exons and 11 introns spanning ~5.7 kb of genomic DNA (Fig. 2 C). All splice junctions were confirmed by sequence analysis of RT-PCR products derived from the wild-type *PF2* transcript. A subsequent search of the *Chlamydomonas* EST database has also identified a cDNA clone (BE056668) whose partial sequence closely matches the predicted sequence of the *PF2* transcript. PCR with gene-specific primers was then used to identify the mutations in two previously isolated *pf2* alleles, *pf2-1* and *pf2-2* (Ebersold et al., 1962; Huang et al., 1982). Sequence analysis of *pf2-1* DNA revealed a single base (G→T) mutation that results in an in-frame stop codon in exon 7 (Fig. 2 C). Interestingly, probes B and C (Fig. 2 A), which contain the DNA encoding exons 1–6, did not detect any transcript on Northern blots of *pf2-1* total RNA (Fig. 2 B), which suggested that the *pf2-1* transcript may be unstable and/or rapidly degraded. Sequence analysis of *pf2-2* DNA revealed a single base (G→A) mutation that altered the donor splice site of exon 1 (Fig. 2 C). Failure to recognize the altered sequence as a splice site would result in translation of the adjacent intron, which contains an in-frame stop codon 30 bp downstream of the altered splice site.

Suppression of flagellar paralysis by *pf2-4*

pf2 mutants belong to a group of bypass suppressor mutations that are capable of restoring motility to paralyzed RS or CP mutants without restoring the missing RS or CP structures (Huang et al., 1982; Piperno et al., 1994). *pf2* mutations also alter the assembly of the DRC polypeptides, which are thought to be regulatory components located between the RS and the dynein arms (Table I; Piperno et al., 1992; Gardner et al., 1994). To test whether *pf2-4* can also act as a suppressor, *pf2-4* was crossed to a paralyzed, RS mutant, *pf14*, and the motility phenotypes of the resulting progeny were analyzed. The *pf2-4 pf14* cells had a motility phenotype that differed from either parent strain or wild-type cells (Table II). The double mutants displayed vigorous flagellar movements, but they could generate little or no forward progress. This type of motility is similar to that seen with other suppressed strains containing defects in the DRC and RS (Huang et al., 1982; Piperno et al., 1992; unpublished data).

Structural defects in the DRC

To determine if the *pf2-4* motility phenotype was also associated with structural defects in the DRC, axonemes were isolated from wild-type and *pf2-4* cells and prepared for EM. Analysis of longitudinal sections with image-averaging procedures revealed a defect in a crescent-shaped structure located close to the second RS, within the 96-nm axoneme repeat (Fig. 3, A and B). This defect is very similar to the defect previously observed in *pf2-1* (Fig. 3 C; Mastronarde et al., 1992; Gardner et al., 1994). The defects can be more clearly seen in the difference plots (Fig. 3, F and G), where the darkened regions represent the statistically significant differences between wild-type and *pf2* axonemes. The missing densities correspond to the structure previously identified as the likely location of the DRC polypeptides (Gardner et al., 1994). Significantly, the recovery of wild-type motility after transforma-

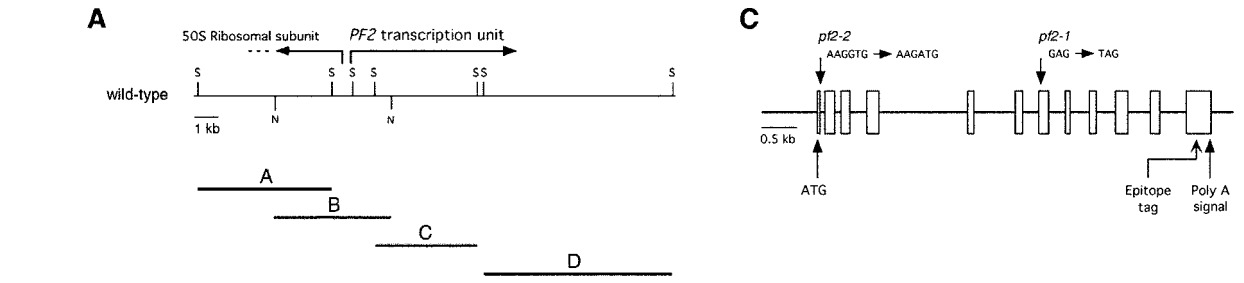

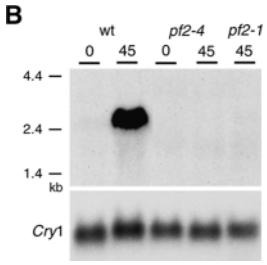

Figure 2. **Analysis of the *PF2* transcription unit.** (A) Partial restriction map of wild-type genomic DNA in the region of the *PF2* transcription unit. Also shown are selected SacI fragments (A, C, and D) and a NotI fragment (B) that were used to map the boundaries of the plasmid insertion and determine the size of the transcription unit. (B) Northern blot loaded with total RNA isolated from wild-type (wt) and *pf2* mutant cells before (0) and 45 min after deflagellation. This blot was hybridized with probe C, which recognized an ~2.5-kb transcript that is up-regulated in wild-type cells and missing in *pf2* mutants. (B, bottom) Loading control. The blot was rehybridized with a *CRY1* probe, which encodes the ribosomal S14 protein subunit (Nelson et al., 1994). (C) Diagram of the intron–exon structure of the *PF2* transcription unit. Open rectangles indicate exons and solid lines indicate introns. The predicted translation start (ATG) site and the putative polyadenylation signal (Poly A) are indicated. Also shown are the single nucleotide alterations that resulted in the *pf2-1* and *pf2-2* mutations, and the location of the epitope tag in exon 12.

tion of *pf2-4* with the wild-type *PF2* gene was also associated with the reassembly of the DRC structure in the rescued strain (Fig. 3 D).

Localization of the PF2 polypeptide and molecular complex formation

Previous studies have shown that *pf2* axonemes lack five axonemal polypeptides known as DRC subunits 3–7 (Table I; Huang et al., 1982; Piperno et al., 1992, 1994). Dikaryon rescue experiments tentatively identified DRC subunit 4 as the gene product of the *PF2* locus (Piperno et al., 1994). To determine if *PF2* encodes a structural component of the axoneme or a polypeptide extrinsic to the axoneme that is required for assembly of the DRC, an epitope-tagged construct was used to rescue the *pf2* mutant phenotype. PF2 is predicted to contain numerous coiled-coil domains throughout its length (Fig. 4 A). The epitope tag was therefore inserted into the 12th exon of the *PF2* gene to avoid possible disruption of the coiled-coil domains and their potential functions (Fig. 2 C; Fig. 4 A). The resulting construct (p9-3HA) is predicted to encode a 60-kD polypeptide with a triple HA epitope tag inserted between aa 458 and 459 of the PF2 sequence. Cotransformation with the epitope-tagged transgene rescued the aberrant motility phenotype of *pf2-4* cells with high efficiency, and the rescued strains swam forward at wild-type velocities (e.g., 127 ± 14 μm/s), demonstrating that the presence of the epitope tag does not interfere with the function of PF2 (Fig. 1 C). Axoneme samples from wild-type, *pf2-4*, and rescued *pf2-4* strains were analyzed on Western blots probed with an antibody directed against the HA epitope. A single polypeptide migrating at ~60 kD was observed exclusively in the epitope-tagged, rescued strain (Fig. 4 B), which indicates that PF2 is a structural component of the isolated axoneme. The size of the epitope-tagged PF2 is consistent with the hypothesis that *PF2* encodes DRC subunit 4 (Piperno et al., 1994).

Mutant and rescued cells were stained with antibodies against the HA epitope to analyze the subcellular distribution of PF2. Analysis of *pf2* mutant and *pf2* rescued cells by differential interference contrast microscopy demonstrated that both strains assemble full-length flagella (Fig. 5, A, C, and E). Staining with the HA antibody revealed that the tagged PF2 is present along the entire length of the flagella in the *pf2-4* rescued strain (Fig. 5, B and D) but missing in control samples (Fig. 5, F and H). The tagged PF2 was also visible in

Table I. **Dynein regulatory complex subunits**

Subunit	Molecular mass[a]	Polypeptide deficiency in[a,b]	Gene product of
	kD		
1	83	*pf3, sup-pf-5*	*PF3*[c]
2	70	*pf3, sup-pf-5*	Unknown
3	62	*pf2, sup-pf-3*	Unknown
4	55	*pf2, sup-pf-3*	*PF2*[c,d]
5	40	*pf2, pf3, sup-pf-3, sup-pf-4, sup-pf-5*	*SUP-PF-4*[b,c]
6	29	*pf2, pf3, sup-pf-3, sup-pf-4, sup-pf-5*	Unknown
7	192	*pf2*	Unknown

[a]Piperno et al., 1994.
[b]Huang et al., 1982.
[c]Putative gene products based on dikaryon rescue (Piperno et al., 1994).
[d]Identified in this work.

Table II. **Strains used in this work**

Strain	Structural defect	Motility phenotype	Reference
Wild-type (137c)	None	Fast forward swimming	Harris, 1989
*nit1*Δ (A54e18)	None	Fast forward swimming	Nelson et al., 1994
pf2-1 (CC1025)	DRC, inner arm region	Slow forward swimming	Ebersold et al., 1962
pf2-2 (*pf2A*, CC2503)	DRC, inner arm region	Slow forward swimming	Huang et al., 1982
pf2-4[a] (9B11)	DRC, inner arm region	Slow forward swimming	This study
pf2-1 rescue	None	Fast forward swimming	This study
pf2-4 rescue	None	Fast forward swimming	This study
arg2	None	Fast forward swimming	Harris, 1989
arg7	None	Fast forward swimming	Harris, 1989
pf2-1 arg2	DRC, inner arm region	Slow forward swimming	This study
pf2-4 arg7	DRC, inner arm region	Slow forward swimming	This study
pf14	Radial spokes	Paralyzed	Piperno et al., 1981
pf2-4 pf14	Radial spokes and DRC	Limited motility[b]	This study

[a]9B11 is a new *pf2* allele identified in this study. The *pf2-3* (*pf2B*) strain (Huang et al., 1982) is no longer available.
[b]See Results.

two spots at the anterior end of the cell in the rescued strain (Fig. 5, B and D). This site corresponds to the predicted location of the two basal bodies. The faint cell body staining seen in *pf2* and wild-type cells (Fig. 5, F and H) appeared to result from autofluorescence, as a similar pattern was observed after treatment with secondary antibody alone.

Based on the high incidence of coiled-coil domains in the predicted tertiary structure of PF2, it is likely that PF2 interacts with other axonemal polypeptides, specifically other components of the DRC and outer doublet microtubules. To identify those polypeptides, isolated axonemes from the HA-tagged strain were treated with varying concentrations of the zero-length cross-linker 1-ethyl-3-(3-dimethylaminopropyl) carbodiimide hydrochloride (EDC) and then analyzed on Western blots. EDC has previously proven useful in the identification of interactions between subunits of several other axonemal structures (for examples see King et al., 1991; Yang et al., 2000). After a 1-h exposure of isolated axonemes to 1 mM EDC, three new bands migrating at ~125, 130, and 145 kD, as well as a number of higher molecular mass (>250 kD) bands, could be detected (Fig. 6). The PF2 cross-linked products did not react on Western blots with antibodies to α- and β-tubulin (Fig. 6). Rather, the sizes of the PF2 cross-linked products suggest instead a close association of PF2 with three polypeptides of ~65, 70, and 85 kD. These results are consistent with the proposal that PF2 is part of a discrete complex of axonemal polypeptides.

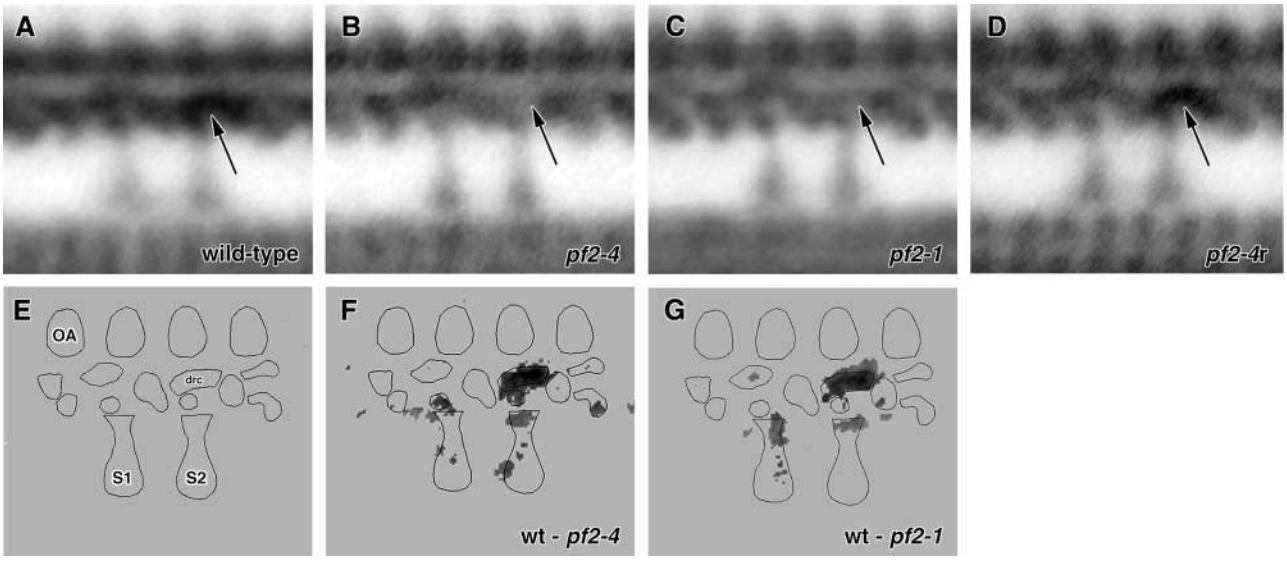

Figure 3. **Structural defects in *pf2* axonemes.** Longitudinal images of wild-type and mutant axonemes were aligned and computer image averaged. Shown here are grand averages of axonemes isolated from (A) wild type, (B) *pf2-4*, (C), *pf2-1*, and (D) a rescued *pf2* strain (*pf2-4*r). The arrows in A–D indicate the region of the 96-nm repeat that is occupied by the DRC structure. (E) Model of axoneme structures within the 96-nm axoneme repeat. The proximal and distal RSs are labeled S1 and S2, respectively; the outer dynein arms (OA) are shown on top, and the DRC is indicated as a crescent-shaped structure above the distal RS (S2). Difference plots between wild type (wt) and *pf2-4* (F), and wt and *pf2-1* (G) demonstrate that the DRC is missing in both mutants. Note that the DRC is restored in the rescued strain, *pf2-4*r (D).

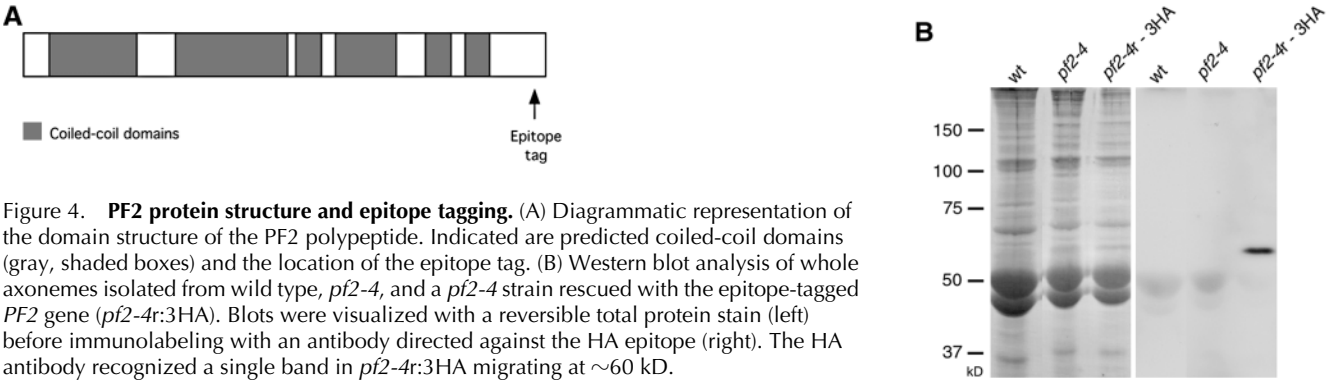

Figure 4. **PF2 protein structure and epitope tagging.** (A) Diagrammatic representation of the domain structure of the PF2 polypeptide. Indicated are predicted coiled-coil domains (gray, shaded boxes) and the location of the epitope tag. (B) Western blot analysis of whole axonemes isolated from wild type, *pf2-4*, and a *pf2-4* strain rescued with the epitope-tagged *PF2* gene (*pf2-4*r:3HA). Blots were visualized with a reversible total protein stain (left) before immunolabeling with an antibody directed against the HA epitope (right). The HA antibody recognized a single band in *pf2-4*r:3HA migrating at ~60 kD.

PF2 encodes the *Chlamydomonas* homologue of Gas11/Gas8

The *Chlamydomonas PF2* gene is predicted to encode a 471-aa polypeptide (Fig. 7 A) with a molecular mass of ~55 kD and pI of 6.66. Database searches reveal that PF2 is closely related to the growth arrest–specific gene product known as *Gas11* in humans and *Gas8* in mice (Whitmore et al., 1998; Yeh et al., 2002). PF2 shares >53% identity and 73% similarity with Gas11 and Gas8 (Fig. 7 A). Significant homology is also observed between PF2 and Gas11/Gas8 orthologues found in zebrafish (*Danio rerio*), flies (*Drosophila melanogaster*), and trypanosomes (*Trypanosoma brucei*) (Fig. 7 A). PF2 homologues have also been identified in ESTs obtained from cow, pig, and schistosomes. Phylogenetic analysis indicates that PF2 is more closely related to the vertebrate Gas11/Gas8 sequences than to the fly or trypanosome homologues (Fig. 7 B). No PF2 homologues have been identified in either yeast or *Caenorhabditis elegans*. However, high levels of *Gas11/Gas8* transcripts have been detected in numerous vertebrate cells and tissues that do not assemble motile axonemes (Whitmore et al., 1998; Yeh et al., 2002; unpublished data). PF2 homologues may therefore have additional functions in differentiated cells of higher organisms (see Discussion).

Discussion

The *PF2* locus encodes an axonemal component required for assembly of the DRC

The CP, RS, and DRC are key elements in a signal transduction pathway that regulates dynein arm activity to produce the complex waveforms characteristic of eukaryotic cilia and flagella (for reviews see Porter and Sale, 2000; Kamiya, 2002). To better understand the role of the individ-

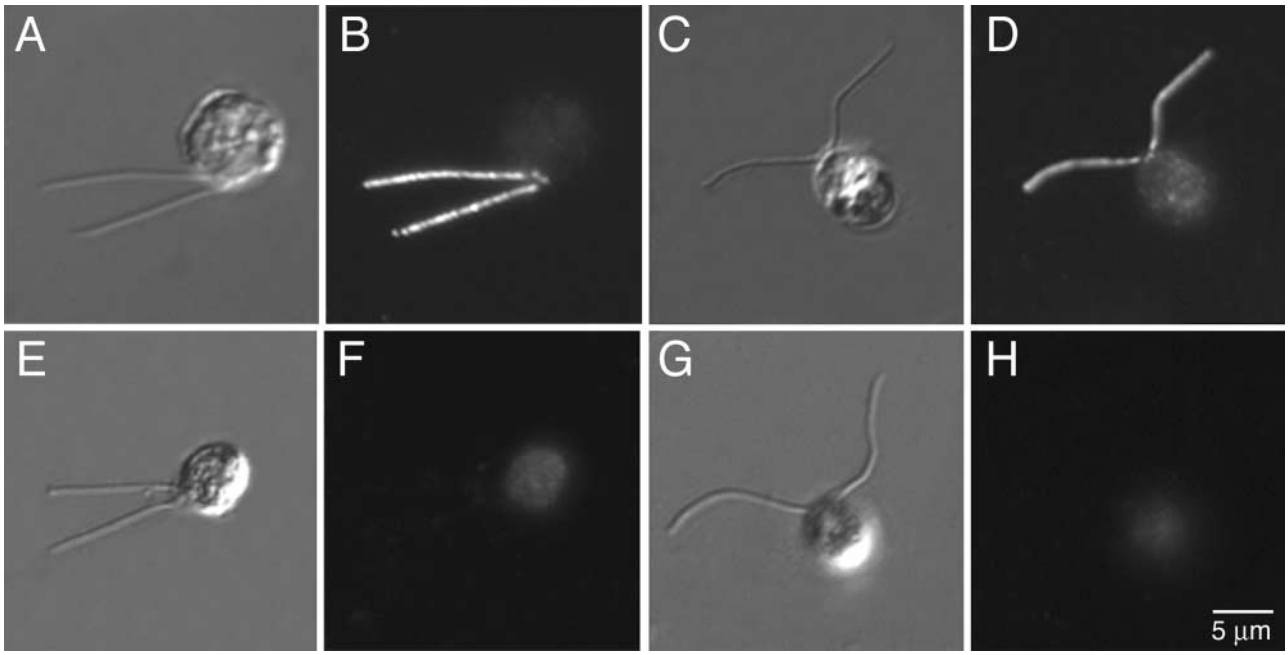

Figure 5. **Localization of the epitope-tagged PF2 protein in *Chlamydomonas* flagella.** The epitope-tagged, rescued strain, *pf2-4*r:3HA, was stained with an antibody against the HA tag and then imaged by differential interference contrast (A and C) or indirect immunofluorescence light microscopy (B and D). The HA-tagged PF2 is present along the entire length of the flagella in *pf2-4*r:3HA cells and can also been seen in two spots in the basal body region (B and D). *pf2-4* mutant (E and F) or wild-type cells (G and H) labeled with the HA antibody or secondary antibody alone (not depicted) show only background cell body autofluorescence.

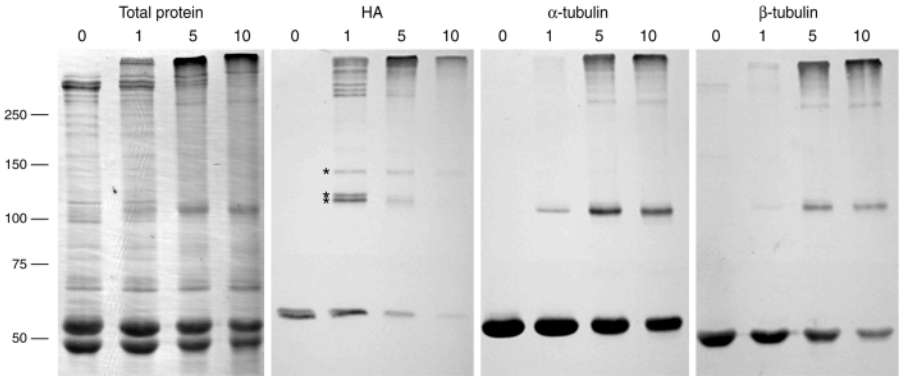

Figure 6. **Identification of polypeptides that interact with PF2.** Axonemes from the HA-tagged *pf2-4* rescued strain were treated with 0, 1, 5, or 10 mM EDC and then used to prepare four identical Western blots. The first blot was stained for total protein. The remaining blots were labeled with antibodies directed against either the HA epitope (HA), α-tubulin (YOL 1/34), or β-tubulin (Tu27B). Asterisks mark three cross-linked products formed as a result of treating the HA-tagged PF2 axonemes with 1 mM EDC.

ual DRC subunits in this pathway, we used insertional mutagenesis strategies to isolate tagged mutations and thereby cloned the *PF2* locus. This is the first DRC gene and gene product to be characterized at both the molecular and cellular levels.

pf2 mutants fail to assemble five of the seven DRC-associated subunits (Table I; Piperno et al., 1994) and display both reduced swimming velocities and aberrant waveforms with reduced shear amplitudes (Brokaw and Kamiya, 1987; Gardner et al., 1994). Our work demonstrates that *PF2* encodes an ~55-kD polypeptide that is uniformly distributed along the length of the axoneme and in the basal body region (Figs. 4 and 5). These results are consistent with the localization of the DRC (Gardner et al., 1994) and a prediction based on dikaryon rescue experiments that *PF2* might encode DRC subunit 4 (Piperno et al., 1994). In addition, transformation of *pf2* mutants with the wild-type *PF2* gene restores both wild-type flagellar motility and the missing DRC structure (Figs. 1 and 3). Thus, PF2 is required for proper assembly of DRC components and the regulation of flagellar motility.

The predicted structure of the PF2 polypeptide contains several coiled-coil domains (Fig. 4) that could play a role in protein–protein interactions. The most likely candidates for such interactions would be other components of the DRC and/or tubulin subunits of the outer doublets. Preliminary experiments using the zero-length cross-linker EDC suggest that PF2 may not directly interact with α- or β-tubulin (Fig. 6), but whether an interaction might be identified using other cross-linking agents remains to be determined. However, a close association between PF2 and at least three polypeptides has been identified, based on the relative mobility of three cross-linked products that react with an antibody specific for the HA-tagged PF2 (Fig. 6). The identities of the three polypeptides are unknown, but their apparent sizes are similar to those reported for three DRC subunits, DRC1, DRC2, and DRC3 (Table I; Piperno et al., 1994). Further confirmation will require the development of specific probes for these other DRC subunits. Nonetheless, these results, together with previous observations that *pf2* axonemes lack five different polypeptides (DRC3–DRC7) (Huang et al.,

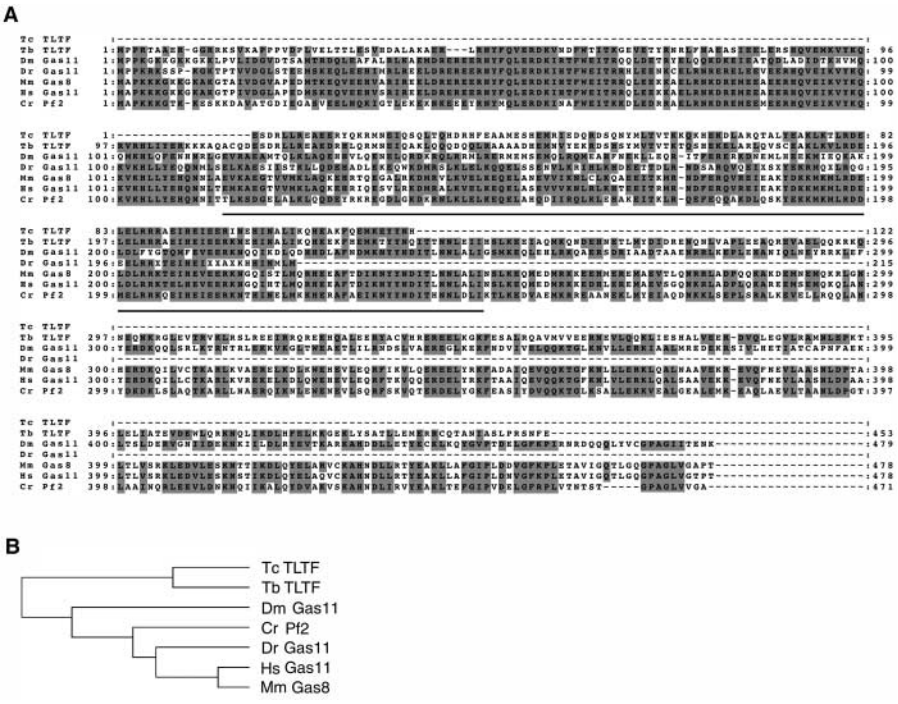

Figure 7. **PF2 homologues.** (A) Clustal W alignment of the deduced amino acid sequence of the *Chlamydomonas reinhardtii* (Cr) *PF2* gene (AY309087–AY309089) with homologues identified by BLAST. The shaded areas represent identical or conservatively substituted amino acids in >50% of the sequences. The underlined region represents a putative microtubule-binding domain identified in the trypanosome and human orthologues (Hill et al., 2000). The abbreviation and GenBank/EMBL/DDBJ accession nos. for the sequences are as follows: *Danio rerio* (Dr), AI584969; *Drosophila melanogaster* (Dm), AE003427 and AA440118; *Homo sapiens* (Hs), AF050079; *Mus musculus* (Mm), U19859; *Trypanosoma bruzi* (Tb), AAB81499; and *Trypanosoma cruzi* (Tc), AQ44061. Gas11, growth arrest–specific 11; Gas8, growth arrest–specific 8. (B) Phylogenetic analysis of the Cr PF2 sequence and its homologues.

1982; Piperno et al., 1992, 1994), indicate that the DRC is a discrete axonemal structure.

The function of PF2-related proteins in other species

Close homologues of PF2 have been found in a variety of organisms (Fig. 7) and include the growth arrest–specific gene product known as Gas8 (mice) or Gas11 (humans) (Brenner et al., 1989; Whitmore et al., 1998; Yeh et al., 2002), the trypanosome protein known as the T lymphocyte triggering factor (TLTF) or trypanin (Vaidya et al., 1997; Hill et al., 2000; Hutchings et al., 2002), and several Gas8/Gas11-related sequences in insects, fish, protozoa, and other mammals. The remarkably high degree of sequence conservation (Fig. 7 A) suggests a highly conserved cellular function.

Gas8 was first described as a gene whose expression in mouse fibroblasts was activated during growth arrest induced by serum starvation (Brenner et al., 1989; Lih et al., 1996). Recent work has shown that both *Gas8* mRNA and Gas8 protein are highly enriched in adult mouse testes (Yeh et al., 2002). Gas8 has been localized along the length of sperm flagella, but it is also found in the apical region of ciliated epithelia that line the respiratory and female reproductive tracts (Yeh et al., 2002). The pattern of localization for Gas8 is similar to that observed for PF2 (Fig. 5) and indicates that both polypeptides are conserved components of motile axonemes.

The human homologue, *Gas11*, was tentatively identified as a candidate tumor suppressor gene based on its location at a chromosome locus (16q24.3) commonly deleted in breast and prostate carcinomas, and the expression of its mouse orthologue during growth arrest (Whitmore et al., 1998). Gas11 has since been localized in developing sperm, but its distribution in other human tissues has not been analyzed (Yeh et al., 2002). Interestingly, however, overexpression of a highly conserved region of Gas11 (aa 115–228; Fig. 7) resulted in the colocalization of a Gas11–GFP fusion protein with the plus ends of cytoplasmic microtubules in both trypanosomes and cultured mammalian cells (Hill et al., 1999, 2000). These observations prompted the suggestion that the conserved region might serve as a novel microtubule-binding domain and that Gas11 may function as a microtubule-specific cytoskeletal linker protein (Hill et al., 1999, 2000). A similar domain is present in PF2 (aa 114–227), but its function is unknown (Fig. 7).

Gas8 and *Gas11* transcripts have previously been detected in a variety of tissues that do not assemble motile axonemes (Whitmore et al., 1998; Yeh et al., 2002). We repeated these experiments using a mouse *Gas8* probe and found high levels of *Gas8* transcripts not only in mouse testis, lung, and brain, but also in heart, liver, and kidney (unpublished data). What might be the origin of *PF2*-related transcripts in these tissues? One possibility might be that all of these tissues contain cells that assemble immotile, primary cilia (see www.wadsworth.org/bms/SCBlinks/cilial1.html). Although primary cilia typically lack the CP, RS, and dynein arms, it is possible that some DRC subunits may have been retained within the axoneme structure. If so, it would be reasonable to identify *PF2*-related transcripts in those tissues that assemble significant levels of primary cilia. Further work is needed to determine if Gas8/Gas11 is found in primary cilia or centrioles in mammalian cells. If present, this may account for the activation of *Gas8* expression observed in growth-arrested fibroblasts (Brenner et al., 1989; Yeh et al., 2002). Previous studies have shown that maximal assembly of primary cilia in these cells is closely correlated with withdrawal from the cell cycle and/or growth to confluence (Tucker et al., 1979; Wheatley et al., 1996). Recent work has also revealed that primary cilia can serve as sensory organelles, relaying signals from receptors in the cilium membrane and thereby allowing cells to monitor their local environment and respond appropriately (Nauli et al., 2003). An exciting possibility is that signals received by primary cilia may influence the growth arrest process (Wheatley et al., 1996; Pazour and Witman, 2003).

An alternative hypothesis would be that the mammalian homologues Gas8 and Gas11 have other, yet unidentified, cytoplasmic functions distinct from their role in the axoneme. The observation that a conserved domain can direct a Gas11 fusion protein to colocalize with the plus ends of microtubules in tissue culture cells (Hill et al., 2000) may support this hypothesis. Additional work is clearly needed to more firmly establish the subcellular distribution of Gas8/Gas11 in mammalian cells.

PF2 is also closely related to a trypanosome protein, trypanin (formerly called TLTF). TLTF was first identified as a polypeptide released by *T. brucei* that triggers $CD8^+$ T lymphocytes to proliferate and secrete γ-interferon (Vaidya et al., 1997). Initial studies of a GFP-tagged TLTF fusion protein suggested that TLTF was localized to the flagellar pocket, a region formed by an invagination of the cell membrane at the site where the flagellum emerges from the cell body (Hill et al., 1999). More recent work has shown that TLTF/trypanin is a component of the trypanosome cytoskeleton (Hill et al., 2000), where it is distributed along the length of the flagellum (similar to both Gas8 and PF2) and may be associated with a region known as the flagellar attachment site (Hutchings et al., 2002).

Interestingly, knockout of trypanin expression by RNA interference has shown that trypanin is required for directional cell motility of the trypanosome (Hutchings et al., 2002). Trypanin(−) mutants do not have paralyzed flagella, but they have lost the ability to coordinate their flagellar beat and thus cannot generate productive cell motility. Analysis by transmission EM failed to identify a clear defect in axoneme structure. However, scanning EM indicated that the flagellum was partially detached from the cell in ∼28% of the trypanin(−) strains as compared with ∼8% in control strains. Hutchings et al. (2002) therefore proposed that trypanin is a novel cytoskeletal linker protein critical for linking the flagellum to the underlying cytoskeleton.

Based on the similarities between PF2 and trypanin, we favor an alternative interpretation of the trypanin(−) phenotype. First, trypanin is likely to be a component of the DRC in the trypanosome axoneme. The EM methods used by Hutchings et al. (2002) to analyze trypanin(−) axonemes would probably not be sensitive enough to resolve subtle defects in DRC structure. The identification of structural defects in *pf2* axonemes required the use of image-averaging

procedures (Mastronarde et al., 1992; Gardner et al., 1994). Second, the apparent defect in flagellar attachment to the cell body could be a consequence of the aberrant flagellar motility in the trypanin(−) cells. This interpretation is consistent with the swimming behavior of the trypanin(−) strains (Hutchings et al., 2002), the motility phenotypes of *pf2* mutants in *Chlamydomonas* (Brokaw and Kamiya, 1987; Mastronarde et al., 1992; Gardner et al., 1994), and the present study.

Role of the DRC and its constituent polypeptides

The absence of a functional PF2 protein results in the inability of *pf2* strains to assemble a major portion of the DRC (Gardner et al., 1994; Piperno et al., 1994). The mutant cells also display an unusual motility phenotype (Brokaw and Kamiya, 1987). When combined with a CP- or RS-associated paralyzed flagellar mutation, *pf2* mutations restore partial flagellar motility without restoring the missing CP or RS structures (Huang et al., 1982; Piperno et al., 1992). The suppression of flagellar paralysis has led to the hypothesis that the DRC is a part of a signal transduction pathway that controls motility by regulating dynein activity (for review see Porter and Sale, 2000). The DRC apparently serves this function by acting as an intermediate in the pathway, receiving signals from the CP/RS structures and then distributing them appropriately to the dynein arms.

We propose that *PF2* encodes a DRC polypeptide that is involved in stabilizing the complex by interacting with other DRC subunits. This proposal is supported by the observations that *pf2* axonemes lack four additional DRC subunits (Piperno et al., 1994), PF2 can be cross-linked to at least three axonemal polypeptides (Fig. 6), and coiled-coil domains are present within the PF2 structure (Fig. 4). We suggest that PF2 serves as a molecular scaffold, whose function is to appropriately localize other components within the axoneme, in a manner similar to that suggested for the CP-associated protein PF6 (Rupp et al., 2001) and the RS-associated protein RSP3 (Gaillard et al., 2001). Other DRC subunits could therefore be positioned to interact with the network of regulatory enzymes and thus regulate motility by controlling the phosphorylation state of key axonemal polypeptides. This model is also consistent with observations indicating that the DRC plays an important role in stabilizing the assembly of specific inner arm isoforms (Gardner et al., 1994; Piperno et al., 1994). Alternatively, PF2 might also serve as a mechanical sensor or molecular spring that senses tension during axonemal bending and thereby influences the activity of nearby dynein isoforms. Future studies to identify and characterize other subunits of the DRC that interact with PF2 will be needed to test these various models.

Materials and methods

Mutant strains and genetic analyses

Strains listed in Table II were maintained as previously described (Rupp et al., 2001). The motility mutant 9B11 was generated by transformation of a *nit1-305* strain with the plasmid pMN24 containing a wild-type copy of the *NIT1* gene (Fernandez et al., 1989). The *NIT1* plasmid was inserted into the *PF2* locus (Fig. 1), and so 9B11 is now known as *pf2-4*. Other strains were obtained from the *Chlamydomonas* Genetics Center.

To determine whether the motility phenotype of 9B11 was linked to the *NIT1* plasmid used as a selectable marker, 9B11 was backcrossed to a *nit*$^-$ strain, and the resulting progeny were analyzed for cosegregation of their motility phenotypes and their ability to grow on selective media. Out of 56 progeny obtained from seven complete octads, 28 were *nit*$^+$ and swam slowly, whereas all 28 *nit*$^-$ strains had wild-type motility.

Isolation of genomic sequence flanking the *NIT1* plasmid

Purification of genomic DNA, restriction enzyme digests, agarose gels, isolation of total RNA, preparation of cDNA, PCR reactions, and Southern and Northern blots were performed as previously described (Rupp et al., 2001). To identify genomic DNA flanking the site of the plasmid insertion, wild-type and 9B11 genomic DNA were analyzed on Southern blots, and a 6.2-kb BamHI fragment unique to 9B11 was identified by hybridization with a 3.2-kb probe derived from the 3′ end of *NIT1*. The 6.2-kb BamHI fragment was recovered by screening a size-fractionated minilibrary with the *NIT1* probe as previously described (Rupp et al., 2001). Positive clones were digested with several restriction enzymes and probed with *NIT1* to identify a unique 0.45-kb NotI/BamHI fragment containing only 9B11 genomic DNA. Southern blot analysis confirmed that this fragment, designated FC-1, was located close to the site of *NIT1* insertion (Fig. 1).

Recovery of the wild-type *PF2* gene

A large-insert, wild-type (21gr), genomic library constructed in λFIX II (Schnell and Lefebvre, 1993) was screened with FC-1 as previously described (Rupp et al., 2001). 13 phage clones were recovered and restriction mapped. Selected subclones were sequenced and analyzed for potential open reading frames as previously described (Rupp et al., 2001). 9.3 kb of genomic sequence has been deposited under GenBank/EMBL/DDBJ accession nos. AY309087–AY309089. An incomplete version of the sequence is also present in the recently released draft of the *Chlamydomonas* genome (http://genome.jgi-psf.org/chlre1/chlre1.home.html).

To place the sequence on the genetic map, a genomic fragment was used to identify a PvuII restriction fragment length polymorphism between two strains, 137c and S1-D2. The fragment was then hybridized to a series of mapping filters containing DNA isolated from tetrad progeny of crosses between multiply marked *C. reinhardtii* strains and S1-D2. The segregation of the PvuII polymorphism was analyzed relative to the segregation of >42 genetic and molecular markers (Porter et al., 1996). The sequence is linked to the molecular marker *CRY1* (~9.4 cM) and the motility mutation *pf2-1* (<5.5 cM).

To test whether any of the clones could rescue the motility defects in *pf2-4* and other *pf2* mutants, *pf2 arg* strains were cotransformed with pARG7.8 (containing a wild-type copy of the *ARG7* gene; Debuchy et al., 1989) and the clone in question. Transformants were selected on media lacking arginine and then screened for recovery of wild-type motility (Rupp et al., 2001).

Construction of an epitope-tagged gene construct

To determine whether PF2 was a structural component of the axoneme, a modified *PF2* gene containing three consecutive HA epitopes was constructed. A 6.9-kb XmaI fragment containing the complete *PF2* transcription unit was subcloned from the rescuing phage clone, λG2, into pUC119 to form the plasmid p9B11-X1.2. A sequence encoding a triple HA epitope (p3HA) was PCR amplified from a second plasmid provided by M. Lavoie and C. Silflow (University of Minnesota, St. Paul, MN) using primers with BstEII restriction sites. A 250-bp product containing the triple HA epitope was ligated into pGEM-T Easy (Promega), released with BstEII, and then religated into a unique BstEII site in p9B11-X1.2, yielding the epitope-tagged *PF2* gene, p9-3HA. Sequence analysis confirmed that the epitope tag was inserted into the 12th exon in the proper orientation and reading frame.

Fractionation of flagella and biochemical analyses

Axonemes were isolated from vegetative cells (Porter et al., 1992; Rupp et al., 2001) and analyzed on either 7.5% polyacrylamide or 5–15% acrylamide, 0–2.4 M glycerol gradient gels using the Laemmli (1970) buffer system. Gels were stained directly or transferred to Immobilon-P (Millipore). Total protein on the blots was visualized with Blot FastStain (Chemicon International). Western blots were probed with a high affinity rat antibody directed against the HA epitope (clone 3F10; Roche Molecular Biochemicals). Immunoreactive bands were detected using an alkaline phosphatase–conjugated secondary antibody (Rupp et al., 2001).

To identify polypeptides that associate with PF2, axonemes from the HA-tagged, *pf2-4* rescued strain were prepared in buffer lacking DTT. Chemical cross-linking was performed by treating axoneme samples with

EDC (Pierce Chemical Co.) for 1 h at room temperature (King et al., 1991). The reaction was terminated by the addition of a 10-fold molar excess of β-mercaptoethanol. Western blots were probed with antisera directed against either the HA epitope, α-tubulin (YOL 1/34; Accurate Chemical Co.), or β-tubulin (Tu27B; a gift of L.I. Binder, Northwestern University, Evanston, IL), and the appropriate secondary antibody.

Electron and light microscopy

Axonemes were prepared for EM as described by Porter et al. (1992). The methods for digitization and image averaging were as previously described (Mastronarde et al., 1992; O'Toole et al., 1995). Analysis of axoneme cross sections indicated that the structural defects in *pf2-4* were similar to those seen previously with *pf2-1*, but potential differences between proximal and distal regions were not examined. Control and HA-tagged strains were prepared for immunofluorescence using an ice-cold methanol fixation protocol described by Sanders and Salisbury (1995). Fixed cells were stained with a primary antibody directed against the HA epitope and an Alexa®488 secondary antibody as previously described (Rupp et al., 2001; Perrone et al., 2003).

We thank members of the Porter laboratory for their support, especially Cathy Perrone. We are also grateful to members of the Lefebvre, Linck, and Silflow laboratories for helpful advice. We extend special thanks to Dave Mitchell (State University of New York Health Sciences Center, Syracuse, NY) for providing the 9B11 strain, Eileen O'Toole for expert assistance with image analysis, Matthew Lavoie for supplying the plasmid encoding the triple HA epitope, Andrew Bostrom for analysis of the *pf2* alleles, and Darryl Kreugger for assistance with EM.

This work was supported by grants from the National Institute of General Medical Sciences (GM-55667) and Minnesota Medical Foundation to M.E. Porter. G. Rupp was supported in part by a National Institutes of Health (NIH) postdoctoral fellowship (F32-GM17901), a training grant from the National Science Foundation for Interdisciplinary Studies on the Cytoskeleton (DIR-9113444), and start-up funds from Southern Illinois University School of Medicine. We also acknowledge the assistance of the Boulder Laboratory for 3-Dimensional Fine Structure, which is supported by NIH grant RR00592.

Submitted: 4 March 2003
Revised: 15 May 2003
Accepted: 21 May 2003

References

Afzelius, B.A. 1995. Role of cilia in human health. *Cell Motil. Cytoskeleton.* 32:95–97.

Brenner, D.G., S. Lin-Chao, and S.N. Cohen. 1989. Analysis of mammalian cell genetic regulation in situ by using retrovirus-derived "portable exons" carrying the *Escherichia coli* lacZ gene. *Proc. Natl. Acad. Sci. USA.* 86:5517–5521.

Brokaw, C.J., and R. Kamiya. 1987. Bending patterns of *Chlamydomonas* flagella: IV. Mutants with defects in inner and outer dynein arms indicate differences in dynein arm function. *Cell Motil. Cytoskeleton.* 8:68–75.

Burgess, S.A., D.A. Carter, S.D. Dover, and D.M. Woolley. 1991. The inner dynein arm complex: compatible images from freeze-etch and thin section methods of microscopy. *J. Cell Sci.* 100:319–328.

Debuchy, R., S. Purton, and J.-D. Rochaix. 1989. The arginosuccinate lyase gene of *Chlamydomonas reinhardtii*: an important tool for nuclear transformation and for correlating the genetic and molecular maps of the ARG7 locus. *EMBO J.* 8:2803–2809.

Ebersold, W.T., R.P. Levine, E.E. Levine, and M.A. Olmsted. 1962. Linkage maps in *Chlamydomonas reinhardtii. Genetics.* 47:531–543.

Fernandez, E., R. Schnell, L.P.W. Ranum, S.C. Hussey, C.D. Silflow, and P.A. Lefebvre. 1989. Isolation and characterization of the nitrate reductase structural gene in *Chlamydomonas reinhardtii. Proc. Natl. Acad. Sci. USA.* 86: 6449–6453.

Fox, L.A., and W.S. Sale. 1987. Direction of force generated by the inner row of dynein arms on flagellar microtubules. *J. Cell Biol.* 105:1781–1787.

Gaillard, A.R., D.R. Diener, J.L. Rosenbaum, and W.S. Sale. 2001. Flagellar radial spoke protein 3 is an A-kinase anchoring protein (AKAP). *J. Cell Biol.* 153: 443–448.

Gardner, L.C., E. O'Toole, C.A. Perrone, T. Giddings, and M.E. Porter. 1994. Components of a "dynein regulatory complex" are located at the junction between the radial spokes and the dynein arms in *Chlamydomonas* flagella. *J. Cell Biol.* 127:1311–1325.

Habermacher, G., and W. Sale. 1997. Regulation of flagellar dynein by phosphorylation of a 138-kD inner arm dynein intermediate chain. *J. Cell Biol.* 136: 167–176.

Hamasaki, T., K. Barkalow, J. Richmond, and P. Satir. 1991. cAMP-stimulated phosphorylation of an axonemal polypeptide that copurifies with the 22S dynein arm regulates microtubule translocation velocity and swimming speed in *Paramecium. Proc. Natl. Acad. Sci. USA.* 88:7918–7922.

Harris, E. 1989. The *Chlamydomonas* Sourcebook. Academic Press, San Diego, CA. 780 pp.

Hill, K.L., N.R. Hutchings, D.G. Russell, and J.E. Donelson. 1999. A novel protein targeting domain directs proteins to the anterior cytoplasmic face of the flagellar pocket in African trypanosomes. *J. Cell Sci.* 112:3091–3101.

Hill, K.L., N.R. Hutchings, P.M. Grandgenett, and J.E. Donelson. 2000. T lymphocyte-triggering factor of African trypanosomes is associated with the flagellar fraction of the cytoskeleton and represents a new family of proteins that are present in several divergent eukaryotes. *J. Biol. Chem.* 275:39369–39378.

Huang, B., Z. Ramanis, and D.J. Luck. 1982. Suppressor mutations in *Chlamydomonas* reveal a regulatory mechanism for flagellar function. *Cell.* 28:115–125.

Hutchings, N.R., J.E. Donelson, and K.L. Hill. 2002. Trypanin is a cytoskeletal linker protein and is required for cell motility in African trypanosomes. *J. Cell Biol.* 156:867–877.

Kamiya, R. 2002. Functional diversity of axonemal dyneins as studied in *Chlamydomonas* mutants. *Int. Rev. Cytol.* 219:115–155.

King, S.J., and S.K. Dutcher. 1997. Phosphoregulation of an inner dynein arm complex in *Chlamydomonas reinhardtii* is altered in phototactic mutant strains. *J. Cell Biol.* 136:177–191.

King, S.M., C.G. Wilkerson, and G.B. Witman. 1991. The Mr 78,000 intermediate chain of *Chlamydomonas* outer arm dynein interacts with α-tubulin in situ. *J. Biol. Chem.* 266:8401–8407.

Laemmli, U.K. 1970. Cleavage of structural proteins during the assembly of the head of bacteriophage T4. *Nature.* 227:680–685.

Lefebvre, P.A., and J.L. Rosenbaum. 1986. Regulation of the synthesis and assembly of ciliary and flagella proteins during regeneration. *Annu. Rev. Cell Biol.* 2:517–546.

Lih, C.-J., S.N. Cohen, C. Wang, and S. Lin-Chao. 1996. The platelet-derived growth factor α-receptor is encoded by a growth-arrest-specific (*gas*) gene. *Proc. Natl. Acad. Sci. USA.* 93:4617–4622.

Mastronarde, D.N., E.T. O'Toole, K.L. McDonald, J.R. McIntosh, and M.E. Porter. 1992. Arrangement of inner dynein arms in wild-type and mutant flagella of *Chlamydomonas. J. Cell Biol.* 118:1145–1162.

Nauli, S.M., F.J. Alenghat, Y. Luo, E. Williams, P. Vassilev, X. Li, A.E. Elia, W. Lu, E.M. Brown, S.J. Quinn, et al. 2003. Polycystins 1 and 2 mediate mechanosensation in the primary cilium of kidney cells. *Nat. Genet.* 33:129–137.

Nelson, J.A.E., P.B. Savereide, and P.A. Lefebvre. 1994. The *Cry1* gene in *Chlamydomonas reinhardtii*: structure and use as a dominant selectable marker for nuclear transformation. *Mol. Cell. Biol.* 14:4011–4019.

Nonaka, S., Y. Tanaka, Y. Okada, S. Takeda, A. Harada, Y. Kanai, M. Kido, and N. Hirokawa. 1998. Randomization of left-right asymmetry due to loss of nodal cilia generating leftward flow of extraembryonic fluid in mice lacking KIF3B motor protein. *Cell.* 95:829–837.

O'Toole, E., D. Mastronarde, J.R. McIntosh, and M.E. Porter. 1995. Computer-assisted analysis of flagellar structure. *Methods Cell Biol.* 47:183–191.

Omoto, C.K., and C. Kung. 1979. The pair of central tubules rotates during ciliary beat in *Paramecium. Nature.* 279:532–534.

Omoto, C.K., I.R. Gibbons, R. Kamiya, C. Shingyoji, K. Takahashi, and G.B. Witman. 1999. Rotation of the central pair microtubules in eukaryotic flagella. *Mol. Biol. Cell.* 10:1–4.

Pazour, G.J., and J.L. Rosenbaum. 2002. Intraflagellar transport and cilia-dependent diseases. *Trends Cell Biol.* 12:551–555.

Pazour, G.J., and G.B. Witman. 2003. The vertebrate primary cilium is a sensory organelle. *Curr. Opin. Cell Biol.* 15:105–110.

Perrone, C.A., D. Tritschler, P. Taulman, R. Bower, B.K. Yoder, and M.E. Porter. 2003. A novel dynein light intermediate chain co-localizes with the retrograde motor for intraflagellar transport at sites of axoneme assembly in *Chlamydomonas* and mammalian cells. *Mol. Biol. Cell.* 14:2041–2056.

Piperno, G., B. Huang, Z. Ramanis, and D.J.L. Luck. 1981. Radial spokes of *Chlamydomonas* flagella: polypeptide composition and phosphorylation of stalk components. *J. Cell Biol.* 88:73–79.

Piperno, G., K. Mead, and W. Shestak. 1992. The inner dynein arms I2 interact with a "dynein regulatory complex" in *Chlamydomonas* flagella. *J. Cell Biol.* 118:1455–1463.

Piperno, G., K. Mead, M. LeDizet, and A. Moscatelli. 1994. Mutations in the "dynein regulatory complex" alter the ATP-insensitive binding sites for inner arm dyneins in *Chlamydomonas* axonemes. *J. Cell Biol.* 125:1109–1117.

Porter, M.E., J. Power, and S.K. Dutcher. 1992. Extragenic suppressors of paralyzed flagellar mutations in *Chlamydomonas reinhardtii* identify loci that alter the inner dynein arms. *J. Cell Biol.* 118:1163–1176.

Porter, M.E., J.A. Knott, L.C. Gardner, D.K. Mitchell, and S.K. Dutcher. 1994. Mutations in the *SUP-PF-1* locus of *Chlamydomonas reinhardtii* identify a regulatory domain in the β-dynein heavy chain. *J. Cell Biol.* 126:1495–1507.

Porter, M.E., J.A. Knott, S.H. Myster, and S.J. Farlow. 1996. The dynein gene family in *Chlamydomonas reinhardtii. Genetics.* 144:569–585.

Porter, M.P., and W.S. Sale. 2000. The 9 + 2 axoneme anchors multiple inner arm dyneins and a network of kinases and phosphatases that control motility. *J. Cell Biol.* 151:F37–F42.

Rupp, G., E. O'Toole, L.C. Gardner, B.F. Mitchell, and M.P. Porter. 1996. The *sup-pf-2* mutations of *Chlamydomonas* alter the activity of the outer dynein arm by modification of the γ-dynein heavy chain. *J. Cell Biol.* 135:1853–1865.

Rupp, G., E. O'Toole, and M.P. Porter. 2001. The *Chlamydomonas PF6* locus encodes a large alanine/proline-rich polypeptide that is required for assembly of a central pair projection and regulated flagellar motility. *Mol. Biol. Cell.* 12:739–751.

Sale, W.S., and P. Satir. 1977. The direction of active sliding of microtubules in *Tetrahymena* cilia. *Proc. Natl. Acad. Sci. USA.* 74:2045–2049.

San Agustin, J.T., and G.B. Witman. 1994. Role of cAMP in the reactivation of demembranated ram spermatozoa. *Cell Motil. Cytoskeleton.* 27:206–218.

Sanders, M.A., and J.L. Salisbury. 1995. Immunofluorescence microscopy of cilia and flagella. *Methods Cell Biol.* 47:163–169.

Sapiro, R., I. Kostetskii, P. Olds-Clarke, G.L. Gerton, G.L. Radice, and J.F. Strauss III. 2002. Male infertility, impaired sperm motility, and hydrocephalus in mice deficient in sperm-associated antigen 6. *Mol. Cell Biol.* 22: 6298–6305.

Schnell, R.A., and P.A. Lefebvre. 1993. Isolation of the *Chlamydomonas* regulatory gene *NIT2* by transposon tagging. *Genetics.* 134:737–747.

Smith, E.F. 2002. Regulation of flagellar dynein by calcium and a role for an axonemal calmodulin and calmodulin-dependent kinase. *Mol. Biol. Cell.* 13: 3303–3313.

Smith, E.F., and W.S. Sale. 1992. Regulation of dynein-driven microtubule sliding by the radial spokes in flagella. *Science.* 257:1557–1559.

Supp, D.M., S.S. Potter, and M. Bruekner. 2000. Molecular motors: the driving force behind mammalian left-right development. *Trends Cell Biol.* 10:41–45.

Tam, L.-W., and P.A. Lefebvre. 1993. Cloning of flagellar genes in *Chlamydomonas reinhardtii* by DNA insertional mutagenesis. *Genetics.* 135:375–384.

Tucker, R.W., C.D. Scher, and C.D. Stiles. 1979. Centriole deciliation associated with the early response of 3T3 cells to growth factors but not to SV40. *Cell.* 18:1065–1072.

Vaidya, T., M. Bakhiet, K.L. Hill, T. Olsson, K. Kristensson, and J.E. Donelson. 1997. The gene for a T lymphocyte triggering factor from African trypanosomes. *J. Exp. Med.* 186:433–438.

Wheatley, D.N., A.M. Wang, and G.E. Strugnell. 1996. Expression of primary cilia in mammalian cells. *Cell Biol. Int.* 20:73–81.

Whitmore, S.A., C. Settasatian, J. Crawford, K.M. Lower, B. McCallum, R. Seshadri, C.J. Cornelisse, E.W. Moerland, A.-M. Cleton-Jansen, A.J. Tipping, et al. 1998. Characterization and screening for mutations of the growth arrest-specific 11 (*GAS11*) and *C16orf3* genes at 16q24.3 in breast cancer. *Genomics.* 53:325–331.

Witman, G.B., J. Plummer, and G. Sander. 1978. *Chlamydomonas* flagellar mutants lacking radial spokes and central tubules. Structure, composition, and function of specific axonemal components. *J. Cell Biol.* 76:729–747.

Woolley, D.M. 1997. Studies on the eel sperm flagellum I. The structure of the inner dynein arm complex. *J. Cell Sci.* 110:85–94.

Yang, P., and W.S. Sale. 2000. Casein kinase I is anchored on axonemal doublet microtubules and regulates flagellar dynein phosphorylation and activity. *J. Biol. Chem.* 275:18905–18912.

Yang, P., L. Fox, R.J. Colbran, and W.S. Sale. 2000. Protein phosphatases PP1 and PP2A are located in distinct positions in the *Chlamydomonas* flagellar axoneme. *J. Cell Sci.* 113:91–102.

Yeh, S.-D., Y.-J. Chen, A.C.Y. Chang, R. Ray, B.-R. She, W.-S. Lee, H.-S. Chiang, S.N. Cohen, and S. Lin-Chao. 2002. Isolation and properties of *Gas8*, a growth arrest-specific gene regulated during male gametogenesis to produce a protein associated with the sperm motility apparatus. *J. Biol. Chem.* 277:6311–6317.